J. Am. Chem. Soc. 1983, 105, 3489-3494

Raman and Infrared Spectra of Binuclear Platinum(II) and Platinum(III) Octaphosphite Complexes. A Characterization of the Intermetallic Bonding

Paul Stein,*[1a] Mark K. Dickson,[1b] and D. Max Roundhill*[1c]

Contribution from the Department of Chemistry, Washington State University, Pullman, Washington 99164. *Received September 7, 1982*

Abstract: Raman and IR spectra of $K_4[Pt_2(pop)_4X_2]$ (X = Cl, Br, I; pop = $P_2O_5H_2^{2-}$) complexes were recorded and the Raman active Pt(III)–Pt(III) stretching frequencies observed at 158, 134, and 110 cm^{-1}. Symmetric Pt–X stretching frequencies were assigned at 304, 224, and 194 cm^{-1}, respectively, while the asymmetric Pt–X frequencies occurred at 295, 195, and 118 cm^{-1}. The Raman spectrum of $[Pt_2(pop)_4]^{4-}$ in aqueous solution was recorded and the Pt(II)–Pt(II) stretching frequency was detected at 116 cm^{-1}. A vibrational analysis, utilizing the X–Pt–Pt–X unit, was performed. This model could reproduce the Raman active vibrations (±2 cm^{-1}) and was sufficient to indicate a strong Pt(III)–Pt(III) single bond and a weak Pt(II)–Pt(II) bond. The Raman spectrum of $[Pt_2(pop)_4CH_3I]^{4-}$ showed ν(Pt–Pt) 156 cm^{-1}, ν(Pt–I) 172 cm^{-1}, and ν(Pt–C) 489 cm^{-1}, the latter frequency shifting to 475 cm^{-1} with a $^{13}CH_3$ isotope. A normal coordinate calculation including the bridging POP atoms gave good reproductions of the Pt–Pt and Pt–X frequencies and predicted an asymmetric ring mode below 200 cm^{-1} that couples with the asymmetric Pt–X stretch. This ring transition was identified in $[Pt_2(pop)_4I_2]^{4-}$ and $[Pt_2(pop)_4CH_3I]^{4-}$ complexes at 178 and 172 cm^{-1}. The ν(Pt–Pt) signal at 116 cm^{-1} in $[Pt_2(pop)_4]^{4-}$ was found to involve a significant contribution of the symmetric ring bending. The $P_2O_5H_2^{2-}$ ligand vibrations were assigned in the IR spectra and the symmetric POP stretch showed a 35-cm^{-1} upshift in the Pt(III) complexes. By use of Badger's rule, an apparent 4% reduction in platinum–platinum separation is calculated for the excited state in $K_4[Pt_2(pop)_4]$.

Although few platinum(III) compounds are known, recent reports of binuclear Pt(III) complexes with Pt–Pt distances between 2.47 and 2.695 Å[2,3] have attracted attention. We have found that binuclear platinum(III) complexes of $[Pt_2(pop)_4X_2]^{4-}$ (X = Cl, Br, I) can be readily prepared by oxidative addition reaction (1) with the binuclear Pt(II) octaphosphite salt $[Pt_2(pop)_4]^{4-}$ (pop = $P_2O_5H_2^{2-}$).[2]

$$[Pt_2(pop)_4]^{4-} + X_2 \rightarrow [Pt_2(pop)_4X_2]^{4-} \qquad (1)$$

Simple MO theory[4] of binuclear complexes of d^7 and d^8 metal ions predicts that these reactions may be facilitated by the formation of a Pt–Pt single bond in the product complex. The binuclear d^8 ion, $[Pt_2(pop)_4]^{4-}$, with orbitals $(d_\sigma)^2(d_{\sigma^*})^2$ has a formal bond order of zero, while a single bond is given to the binuclear d^7 ions, $[Pt_2(pop)_4X_2]^{4-}$, with a filled $(d\sigma^2)$ orbital. The Pt–Pt distance in $K_4[Pt_2(pop)_4Cl_2]$ is 2.695 (1) Å which is considerably shorter than that of 2.925 (1) Å in $K_4[Pt_2(pop)_4]\cdot 2H_2O$.[5] Magnetic measurements indicate these complexes are diamagnetic. The ^{31}P and ^{195}Pt NMR spectra show these complexes are stable in solution although second-order splittings of the resonances complicate the evaluation of a quantitative description of the Pt–Pt interactions.

Raman spectral measurements in aqueous solution have been reported for the $[Pt_2(pop)_4X_2]^{4-}$ ions, giving ν(Pt–Pt) at 158, 134, and 110 cm^{-1}, and for $[Pt_2(pop)_4]^{4-}$ at 116 cm^{-1}.[6] While ν(Pt–Pt) provides a sensitive monitor of the Pt–Pt interaction, the influence of the ligands obscures a direct correlation to Pt–Pt bonding. For the purpose of estimating the bond strengths in both the binuclear platinum(II) and platinum(III) complexes, we have collected the Raman and IR spectral data of $[Pt_2(pop)_4]^{4-}$, $[Pt_2(pop)_4X_2]^{4-}$ (X = Cl, Br, I) and $[Pt_2(pop)_4CH_3I]^{4-}$. Application of a normal coordinate analysis delineates the ligand contributions to the Pt–Pt stretching modes. A characterization of binuclear platinum(II) and platinum(III) bond strengths will significantly improve our understanding of the interactions in these molecules and possibly lead to better predictions of their chemistries.

The electronic spectral properties of these complexes have been investigated. Intense absorptions for $[Pt_2(pop)_4]^{4-}$ (367 nm)[7] and $[Pt_2(pop)_4X_2]^{4-}$ (310–460 nm) have been assigned to $5d_{z^2}(\sigma^*) \rightarrow 6p_z(\sigma)$[8,9] and $5d_{z^2}(\sigma) \rightarrow 5d_{z^2}(\sigma^*)^2$ transitions. Electronically similar binuclear rhodium(I) and rhodium(II) ions $[Rh_2b_4]^{2-}$ and $[Rh_2b_4X_2]^{2+}$ (b = 1,3-diisocyanopropane)[10,11] show comparative absorptions. Much interest has been afforded to these d^8 binuclear platinum(II) and rhodium(I) complexes which show efficient phosphorescence with vibrational progressions at 139 and 147 cm^{-1}. These vibrations have been assigned to the metal–metal stretching frequencies in the excited state and they occur with an increase in the metal–metal bond strength over that of the ground state. The Rh–Rh stretching frequencies, 79 cm^{-1} for the ground state and 144 cm^{-1} for the triplet level, have been observed for the binuclear rhodium(I) complex by Raman spectroscopy.[12]

We now report our vibrational analysis for the binuclear platinum complexes and suggest that it may serve as a point of reference in analyzing similar face-centered binuclear or oligomeric structures.[13]

Experimental Section

Complexes $K_4[Pt_2(pop)_4]\cdot 2H_2O$, $K_4[Pt_2(pop)_4X_2]$ (X = Cl, Br, I), and $K_4[Pt_2(pop)_4CH_3I]$ were prepared by published procedures.[2,5,7] The compound $K_4[Pt_2(pop)_4{}^{13}CH_3I]$ was prepared in a similar manner[2] except

---

(1) (a) Present address: Department of Chemistry, Duquesne University, Pittsburgh, PA 15282. (b) Shell Development Co. Houston, TX 77001. (c) Department of Chemistry, Tulane University, New Orleans, LA 70118.

(2) Che, C. M.; Schaefer, W. P.; Gray, H. B.; Dickson, M. K.; Stein, P.; Roundhill, D. M. *J. Am.* Chem. *Soc.* **1982**, *104*, 4253–4255.

(3) Muraveiskaya, G. S.; Orlova, V. S.; Evstaf'eva, O. N. *Russ. J. Inorg. Chem.* **1974**, *19*, 1030–1035. Orlova, V. S.; Muraveiskaya, G. S.; Evstaf'eva, O. N. *Ibid.* **1975**, *20*, 1340–1346. Muraveiskaya, G. S.; Kukina, G. A.; Orlova, V. S.; Evstaf'eva, O. N.; Porai-Koshits, M. A. *Dokl. Akad. Nauk SSSR* **1976**, *226*, 596–599. Cotton, F. A.; Falvello, L. R.; Han, S. *Inorg. Chem.* **1982**, *21*, 1709–1710. Cotton, F. A.; Falvello, L. R. han, S. *Inorg. Chem.* **1982**, *21*, 2889–2891. Hollis, L. S.; Lippard, S. J. *J. Am. Chem. Soc.* **1981**, *103*, 6761–6763.

(4) Mann, K. R.; Lewis, N. S.; Williams, R. M.; Gray, H. B.; Gordon, J. G. *Inorg. Chem.* **1978**, *17*, 828–834.

(5) Filomena Dos Remedios Pinto, M. A.; Sadler, P. J.; Neidle, S.; Sanderson, M. R.; Subbiah, A. *J. Chem. Soc., Chem. Commun.* **1980**, 13–15.

(6) Stein, P. In "Raman Spectroscopy; Linear and Nonlinear"; Lascombe, J., Huong, P. V., Eds.; Wiley Heyden Publishers, 1982; pp 651–652.

(7) Sperline, R. P.; Dickson, M. K.; Roundhill, D. M. *J. Chem. Soc., Chem. Commun.* **1977**, 62–63.

(8) Fordyce, W. A.; Brummer, J. G.; Crosby, G. A. *J. Am. Chem. Soc.* **1981**, *103*, 7061–7064.

(9) Che, C. M.; Butler, L. G., Gray, H. B. *J. Am. Chem. Soc.* **1981**, *103*, 7796–7797.

(10) Lewis, N. S.; Mann, K. R.; Gordon, J. G., II; Gray, H. B. *J. Am. Chem. Soc.* **1976**, *98*, 7461–7463.

(11) Rice, S. F.; Gray, H. B. *J. Am. Soc.* **1981**, *103*, 1593–1595.

(12) Dallinger, R. F.; Miskowski, V. M.; Gray, H. B.; Woodruff, W. H. *J. Am. Chem. Soc.* **1981**, *103*, 1595–1596.

(13) Dickson, M. K.; Fordyce, W. A.; Appel, D. M. Alexander, K.; Stein, P.; Roundhill, D. M. *Inorg. Chem.* **1982**, *21*, 3857–3858.

0002-7863/83/1505-3489$01.50/0

Table I. Vibrational Frequencies (cm^{-1}) of $[Pt_2(pop)_4]^{4-}$ and $[Pt_2(pop)_4X_2]^{4-}$

$[Pt_2(pop)_4]^{4-}$	$[Pt_2(pop)_4Cl_2]^{4-}$	$[Pt_2(pop)_4Br_2]^{4-}$	$[Pt_2(pop)_4I_2]^{4-}$	$[Pt_2(pop)_4CH_3I)]^{4-}$	assignments
			IR		
1329	1270	1270	1270	1270	POH bend
1085	1060	1092	1090	1083	PO_{term} str
910	940	930	920	915	PO_{term} str
695	730	730	728	725	POP str
520	516	520	515	520	PO_2 bend
442	455	456	452	453, 475	PO_2 bend
360	359	357	357	356	ring bending
335	335	336	335	336	Pt-P str
308	320	318	318	320	ring bending
	295	195	118 (178)[d]	115 (172)[d]	Pt-X str
278	275	283	281	287	ring bending
241	237	237	237	239	ring bending
			Raman		
	304	224	195	172	Pt-X str[c]
232	235		*b*	*b*	ring bending
116	158	134	110[a]	156	Pt-Pt str
	112	95	*b*	*b*	Pt-Pt-X bending

[a] Overtones are shown in Figure 3 at 218 cm^{-1} and 326 cm^{-1}. [b] Not observed. [c] Pt-CH_3 in $[Pt_2(pop)_4CH_3I]^{4-}$ is observed at 489 cm^{-1} as shown in Figure 5. [d] Assigned to ring bending but contain significant Pt-I str contribution (see Table II).

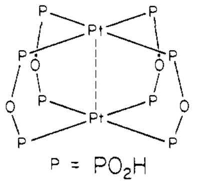

Figure 1. Schematic drawing of the $[Pt_2(pop)_4]^{4-}$ structure. The $[Pt_2(pop)_2X_2]^{4-}$ structures have, in addition, Pt-X units.

that $^{13}CH_3I$ (90 atom % $^{13}CH_3I$ supplied by MSD Isotopes) was used. Infrared spectra were obtained as Vaseline mull films on a polyethylene plate in an evacuated sample chamber of a Perkin-Elmer FIS3 spectrometer. Deuteration of $K_4[Pt_2(pop)_4]$ was achieved by carrying out the synthesis in D_2O solvent. Samples for Raman spectroscopy were prepared as saturated aqueous solutions. Raman spectra of the binuclear Pt(III) complexes were obtained with an argon ion 554 Control laser. A 171 Spectrophysics krypton ion laser was used for the binuclear Pt(II) sample.

Results and Discussion

1. Vibrational Symmetries. In analyzing the present vibrational data, it is useful to begin with the structure in Figure 1 which gives the atomic arrangement for the ion $[Pt_2(pop)_4]^{4-}$ and shows fourfold symmetry about the Pt-Pt axis. Twenty seven normal modes are classified in the D_{4h} point group:

$$\Gamma = 4A_{1g} + 1A_{2g} + 3B_{1g} + 2B_{2g} + 4E_g + 1A_{1u} + 3A_{2u} + 1B_{1u} + 3B_{2u} + 5E_u$$

The A_{2u} and E_u type vibrations involve both P-O and Pt-P stretches and ring bending modes and are infrared active. Raman active vibrations involving platinum motions transform with A_{1g} or E_g symmetry. The $[Pt_2(pop)_4X_2]^{4-}$ ions give additional vibrations due to Pt-X linkages as classified:

$$\Gamma = 1A_{1g} + 1E_g + 1A_{2u} + 1E_u$$

Despite the PtPOPPt units being puckered and the PO_2H groups reducing the symmetry from D_{4h}, Figure 1 is useful in analyzing the infrared and Raman active vibrations. A list of number and descriptions of the expected modes are given as follows:

A_{1g}	E_g	A_{2u}	E_u	description
1	1	1	1	P-O-P stretch
1	1	1	1	Pt-P stretch
1	2	1	3	ring bending
1	0	0	0	Pt-Pt stretch
1	0	1	0	Pt-X stretch
0	1	0	1	Pt-X bend

As seen, the Pt-Pt stretching coordinate occurs only in A_{1g} symmetry and ν(Pt-Pt) is expected to be a mixture of this coordinate, the symmetric Pt-X, and bridging ligand coordinates. The A_{1g} and A_{2u} type vibrations can couple in $[Pt_2(pop)_4CH_3I]^{4-}$ where the symmetry reduces to C_{4v}.

2. Bridging Ligand Vibrations. The IR spectra of the ions $[Pt_2(pop)_4]^{4-}$ and $[Pt_2(pop)_4X_2]^{4-}$ are dominated by vibrational modes from the $P_2O_5H_2^{2-}$ units. Their frequencies are listed in Table I. The $[Pt_2(pop)_4X_2]^{4-}$ complexes show nearly equivalent sets of frequencies which are interpreted as evidence for little variation of their bridging units. While a comparison between the binuclear Pt(III) and Pt(II) complexes show vibrational frequency shifts, the vibrational patterns remain the same. The P-O-P stretching and PO_2H group vibrations are expected above 400 cm^{-1} while the ring bending modes and the Pt-X stretches occur below 400 cm^{-1}.

Symmetric and asymmetric P-O-P stretches have been assigned at 670 and 915 cm^{-1} in pyrophosphites,[14] and at 710-750 and 910-1025 cm^{-1} in diphosphates.[15] The asymmetric P-O-P stretch (A_{2u}) is obscured by the PO_2H vibrations. The symmetric P-O-P stretch (E_u) is observed at 695 cm^{-1} in $[Pt_2(pop)_4]^{4-}$ and at 730 cm^{-1} in the $[Pt_2(pop)_4X_2]^{4-}$ complexes. Although the measured P-O distances in $[Pt_2(pop)_4]^{4-}$ and $[Pt_2(pop)_4Cl_2]^{4-}$ are 1.61 ± 0.01 Å,[2,5] a 35-cm^{-1} shift to higher frequency is observed for the symmetric P-O-P stretch between the Pt(II) and Pt(III) ions. This difference can be ascribed to kinematic alterations which arise from a change in the POP bridging angles and does not indicate potential energy differences in the $P_2O_5H_2^{2-}$ bridge. A comparison of the $K_4[Pt_2(pop)_4]\cdot 2H_2O$ and $K_4[Pt_2(pop)_4Cl_2]$ crystal structures indicates an approximate 8-10° change in the POP angle which apparently accompanies the change in Pt-Pt distance.[16] An increase in the symmetric P-O-P stretching and decrease in the asymmetric P-O-P stretching frequencies of ~40 cm^{-1} are predicted with this angle change.

The PO_2H vibrations involve P-O stretches, PO_2 bends, and POH bending. The latter is identified at 1320 cm^{-1} in $[Pt_2(pop)_4]^{4-}$ and at 1270 cm^{-1} in the $[Pt_2(pop)_4X_2]^{4-}$ complexes, which shift to lower frequency (~300 cm^{-1}) in the perdeuterated complexes. The symmetric and asymmetric P-O_{term} stretches occur at 1100

---

(14) Ebert, M.; Kawan, L.; Pelikanova, M. *Collect. Czech. Chem. Commun.* **1978**, *43*, 3317-3323 and references therein.

(15) Palmer, W. G. *J. Chem. Soc.* **1961**, 1552-1562. Steger, E.; Leukroth, G. *Z. Anor. Allg. Chem.* **1960**, *303*, 169-176. Muck, A.; Petri, F. *Z. Chem.* **1971**, *11*, 29-30. Etcheverry, S. B.; Baran, E. S. *Z. Anorg. Allg. Chem.* **1971**, *457*, 197-202.

(16) An idealized model where all Pt-Pt-P angles are 90° and all bridging ligand distortion is accommodated by changes in the P-O-P angle was assumed in the calculations of section 3b, giving a 15° change in P-O-P angle between Pt(II)-Pt(II) and Pt(III)-Pt(III) complexes. Actually the angle change is somewhat smaller (~8°) and there is also some increase ~1-2°) in the Pt-Pt-P angles above 90° for the complex $K_4[Pt_2(pop)_4Cl_2]$ (Schaefer, W. P., personal communication).

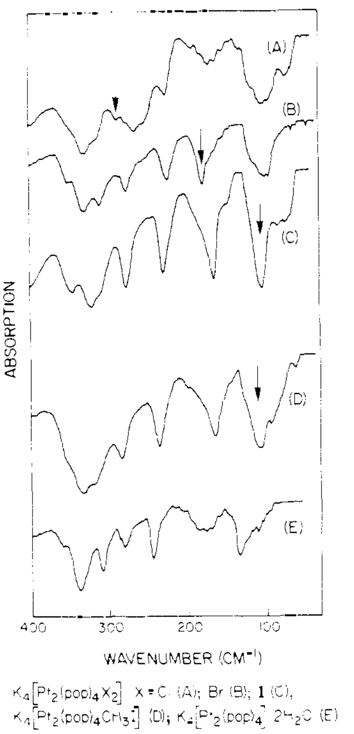

Figure 2. Far-infrared spectra of binuclear platinum(II) and platinum(III) complexes $K_4[Pt_2(pop)_4X_2]$, $K_4[Pt_2(pop)_4CH_3I]$, $K_4[Pt_2(pop)_4]\cdot 2H_2O$. The marked (↑) signals correspond to the Pt–X modes.

and 910 cm^{-1} and are characteristic of a hybridized PO_2 unit without a well-defined P═O bond, which is usually observed above 1200 cm^{-1}.[17] Partial double-bonded $P{-}O_{term}$ units are also suggested by the X-ray data which give $P{-}O_{term}$ distances in the range 1.51–1.55 Å.[16] The PO_2H vibrational bands are broad and may indicate disorder in the hydrogen positions. The vibrations at ~525 and 450 cm^{-1} are compared with PO_2 bending frequencies observed in phosphites and pyrophosphites.[18] These modes are not expected to influence the Pt–Pt stretching frequencies significantly.

Infrared assignments below 400 cm^{-1} are more tentative, although the Pt–X frequencies can be confidently identified at 295, 195, and 118 cm^{-1} for $[Pt_2(pop)_4X_2]^{4-}$ (X = Cl, Br, I). We assign the 335–336-cm^{-1} bands to the Pt–P (E_u) stretch as compared to the range 310–360 cm^{-1} for complexes $PdX_2(PMe_3)_2$.[19] The far-infrared spectra of our complexes, given in Figure 2, show intense lines at 178 and 172 cm^{-1} for $[Pt_2(pop)_4I_2]^{4-}$ and $[Pt_2(pop)_4CH_3I]^{4-}$ in addition to the Pt–I stretches; these vibrations are assigned to asymmetric (A_{2u}) ring-bending vibrations. Their intensity may be attributed to mixing with the Pt–I motions.

3. Pt–Pt and Pt–X Vibrations. The Raman spectra of the $[Pt_2(pop)_4X_2]^{4-}$ ions shown in Figure 3 and that of $[Pt_2(pop)_4]^{4-}$ shown in Figure 4 are characterized in aqueous solution by intense signals between 110 and 158 cm^{-1} and are assigned to the Pt–Pt stretching frequencies. A weaker signal in the ions $[Pt_2(pop)_4X_2]^{4-}$ at 304, 224, and 194 cm^{-1} is due to the symmetric Pt–X stretch. Depolarization ratios show these signals to be polarized. The $[Pt_2(pop)_4Cl_2]^{4-}$ and $[Pt_2(pop)_4Br_2]^{4-}$ ions have broad bands which are depolarized and are assigned to E_g ring bending and Pt–Pt–X bending modes. The band at 232 cm^{-1} in $[Pt_2(pop)_4]^{4-}$ may be the corresponding E_g ring mode or possibly an overtone of ν(Pt–Pt) at 116 cm^{-1}. Modes due to the phosphorus ligands are not observed in these spectra.

The intense ν(Pt–Pt) signal in $[Pt_2(pop)_4I_2]^{4-}$ is attributed to a preresonance enhancement with the σ–σ^* excitaion at 438 nm. The relative intensity of ν(Pt–Pt) in $[Pt_2(pop)_4I_2]^{4-}$ against that in $[Pt_2(pop)_4Cl_2]^{4-}$ is approximately 140 times, and the appearance of the two ν(Pt–Pt) overtones characterize the resonance effect in the $[Pt_2(pop)_4I_2]^{4-}$ ion. These overtone frequencies (218 and 326 cm^{-1}) indicate a reasonably harmonic mode for ν(Pt–Pt).

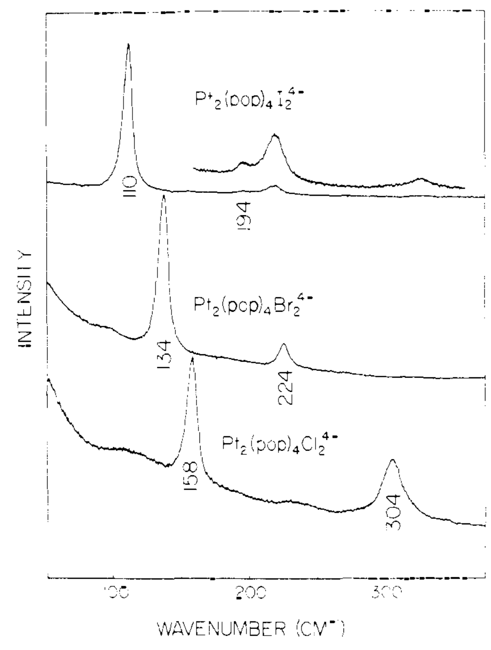

Figure 3. Raman spectra are shown for ~2-mM solutions of $[Pt_2(pop)_4X_2]^{4-}$ (X = Cl, Br, I) in H_2O, using 5145-Å laser excitation. An arbitrary intensity scale is given with each spectrum. The relative intensities of ν(Pt–Pt) are 1:6:143. Intensities of ν(Pt–Pt) are measured (not shown) against the 932-cm^{-1} signal in solutions with $NaClO_4$. An intensity ratio of 0.38 occurs in a solution of 7.8×10^{-5} M $[Pt_2(pop)_4I_2]^{4-}$ vs. 0.8 M $NaClO_4$. Relative intensities of ν(Pt–Pt) with 4880-Å laser excitation are 1.3:8.1:314.

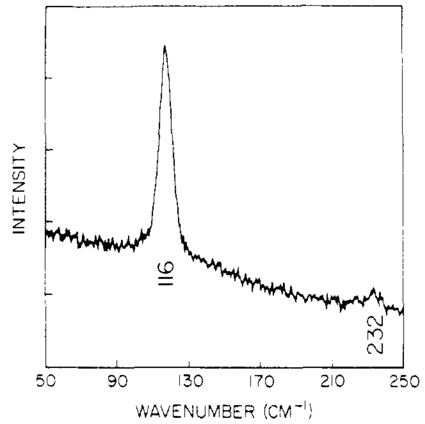

Figure 4. Raman spectrum of ~5-mM aqueous solution of $[Pt_2(pop)_4]^{4-}$, using 4067-Å laser excitation.

The ν(Pt–Pt) and ν(Pt–X) stretches are now analyzed by normal coordinate calculations both with and without the bridging units. A comparison of these results allows a realization of the influence of the bridging units.

(a) Vibrational Analysis of the X–Pt–Pt–X Unit. A simple analysis is offered to estimate the difference in Pt–Pt bond strength between the binuclear Pt(II) and Pt(III) complexes. We find that a linear four-atom unit, X–Pt–Pt–X, is sufficient to reproduce ν(Pt–Pt) and symmetric ν(Pt–X) observed for the $[Pt_2(pop)_4X_2]^{4-}$ ions. An analytical solution has been obtained for ν(Pt–Pt) and the symmetric ν(Pt–X) in terms of three force constants, K(Pt–Pt), K(Pt–X), and I(Pt–Pt; Pt–X). Details are given in the Appendix and frequencies are shown in Table II. Although a unique fit is not possible, a reasonable solution can be chosen with K(Pt–Pt) = 1.7 mdyn/Å, I(Pt–Pt; Pt–X) ≃ 0.16 mdyn/Å, and K(Pt–X) = 1.65, 1.45, and 1.2 mdyn/Å for X = Cl, Br, and I, respectively. When the K(Pt–Pt) force constants are assumed to be linearly

---

(17) Bellamy, L. J.; Beecher, L. *J. Chem. Soc.* **1952**, 475–483.

(18) Tsuboi, M. *J. Am. Chem. Soc.* **1957**, *79*, 1351–1354.

(19) Park, P. J. D.; Hendra, P. J. *Spectrochim. Acta, Part A* **1969**, *25A*, 909–916.

Table II. Observed and Calculated Frequencies and Force Constants of Binuclear Platinum Complexes

A. Normal Modes with Pt–Pt and Pt–X Contributions

		frequency, cm^{-1}		PED,[a] %		
compd	symbol[b]	obsd	calcd[d]	Pt–X	Pt–Pt	bridge[c]
$[Pt_2(pop)_4Cl_2]^{4-}$	A_{1g}	304	304 (304)	78	4	1
		158	153 (157)	1	69	25
	A_{2u}	295	285 (304)	85		1
			154	1		85
$[Pt_2(pop)_4Br_2]^{4-}$	A_{1g}	224	218 (222)	77	22	10
		134	132 (134)	17	51	18
	A_{2u}	195	201 (206)	78		16
			143	17		67
$[Pt_2(pop)_4I_2]^{4-}$	A_{1g}	194	187 (195)	49	47	18
		110	107 (109)	45	26	9
	A_{2u}	178	171 (161)	37		56
		118	121	60		22
$[Pt_2(pop)_4CH_3I]^{4-}$	A_1	489[e]	488[e]	93[e]	1	1
		172	177	48	35	34
		156	159	0	24	57
		115	116	57	12	16
$[Pt_2(pop)_4]^{4-}$	A_{1g}	116	115 (116)		38	58
	A_{2u}		162			89

B. Additional Modes for the A_{1g} and A_{2u} Symmetries of the $[Pt_2(pop)_4X_2]^{4-}$ Complexes (X = Cl, Br, and I) and $[Pt_2(pop)_4]^{4-}$

symbol	$[Pt_2(pop)_4]^{4-}$ calcd, cm^{-1}	$[Pt_2(pop)_4X_2]^{4-}$ calcd, cm^{-1}	$[Pt_2(pop)_4CH_3I]^{4-}$ calcd, cm^{-1}	assignments
A_{1g}	696	758	719	P–O stretch
	403	385	411	Pt–P stretch
	292	294	295	ring bending
A_{2u}	963	923	958	P–O stretch
	372	372	376	Pt–P stretch

C. Force Constants[f] (mdyn/A)

$Pt(III)_2$		$Pt(III)_2$ and $Pt(III)_2$	
K(Pt–Cl)	1.54	K(P–O)	4.0
K(Pt–Br)	1.36	K(Pt–P)	2.2
K(Pt–I)	1.03	K(Pt–Pt)	0.3[g]
K(Pt–C)	2.03	K(Pt–Pt)	1.2[h]
I(Pt–Pt; Pt–X)	0.16	H(Pt–P–O)	0.39
I(P–Pt–P; Pt–X)	0.10	H(P–O–P)	0.47
H(C–C–H)	0.425	H(P–Pt–P)	0.28
H(H–C–H)	0.35		

[a] Diagonal potential energy distribution. [b] D_{4h} symmetry for $[Pt_2(pop)_4]^{4-}$ and $[Pt_2(pop)_4X_2]^{4-}$; C_{4v} symmetry for $[Pt_2(pop)_4CH_3I]^{4-}$. [c] The Pt–Pt–P, P–O–P, and Pt–P–O bending contributions. [d] Calculated frequencies in parentheses were determined by using only the X–Pt–Pt–X unit (see text) and Appendix. [e] Pt–CH_3 str; with $[Pt_2(pop)_4{}^{13}CH_3I]^{4-}$ the Pt–$^{13}CH_3$ str is 475 exptl and 476 calcd. [f] See Appendix for four-atom calculation. [g] For $[Pt_2(pop)_4]^{4-}$. [h] For $[Pt_2(pop)_4X_2]^{4-}$.

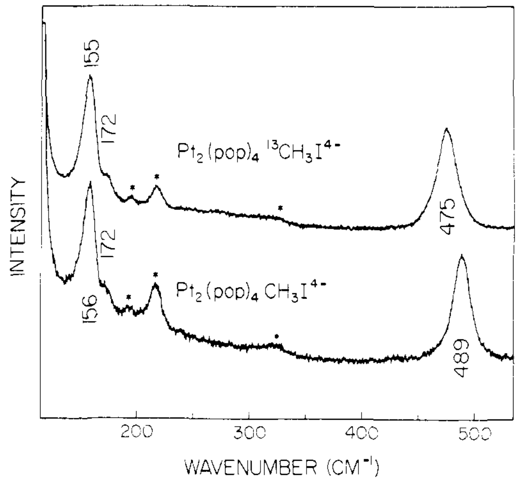

Figure 5. Raman spectra of $[Pt_2(pop)_4CH_3I]^{4-}$ and $[Pt_2(pop)_4{}^{13}CH_3I]^{4-}$ in ~2-mM aqueous solutions are shown. Signals from trace amounts of $[Pt_2(pop)_4I_2]^{4-}$, <5% as determined by ^{31}P NMR measurements, are also observed and indicated by astericks. Laser excitation is 5145 Å.

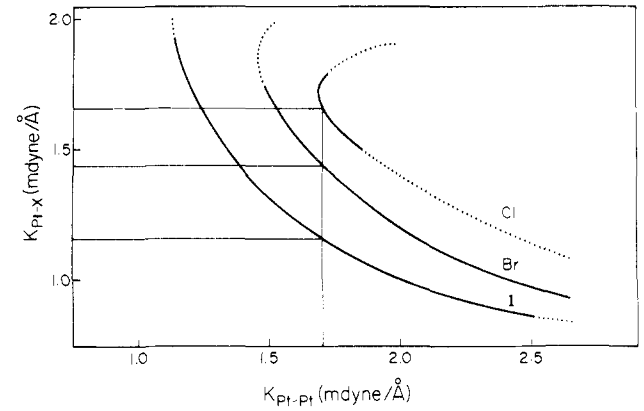

Figure 6. Force fields for $[Pt_2(pop)_4X_2]^{4-}$ (X = Cl, Br, I): (–) give regions for $0.1 < I_{XX'} < 0.4$, (···) give $I_{XX'} > 0.4$, and (- -) give $I_{XX'} < 0.1$. An alternative solution for $[Pt_2(pop)_4Cl_2]^{4-}$ with $K_{PtPt} = 1.7$ mdyn/Å gives $K_{PtCl} = 1.74$ mdyn/Å and $I_{PtX} = 0.31$ mdyn/Å.

related to the Pt–Pt bond strengths, a comparison between binuclear Pt(II) and Pt(III) complexes can be accomplished. A single two-atom calculation for $[Pt_2(pop)_4]^{4-}$ reproduces ν(Pt–Pt) 116 cm^{-1} and gives K(Pt–Pt) = 0.77 mdyn/Å for this complex. Here K(Pt–Pt) corresponds to the sum of the restoring forces that arise from direct Pt–Pt interaction and those which originate from the bridging ligands. Thus, K(Pt–Pt) does not directly correlate with the homometallic bond strengths. The bridging contributions are eliminated in ΔK(Pt–Pt), the difference between K(Pt–Pt) for the binuclear Pt(III) and Pt(II) complexes. Since the same bridging ligands are compared and appear similar, as witnessed by the X-ray data and the IR spectra, their interaction may reasonably be assumed not to be markedly different. This analysis gives ΔK(Pt–Pt) = 0.93 mdyn/Å and indicates an increase of the Pt–Pt bond strength in the binuclear Pt(III) complexes.

(b) Analysis Including the Bridge A_{1g} and A_{2u} Vibrations. The Pt–Pt and Pt–X stretching frequencies are now analyzed with the bridging ligands included. By use of the atomic arrangement in Figure 1 with Pt–P and P–O distances of 2.35 and 1.61 Å, the A_{1g} and A_{2u} symmetry vibrations of $[Pt_2(pop)_4]^{4-}$ and $[Pt_2(pop)_4X_2]^{4-}$ complexes have been analyzed. A Pt(II)–Pt(II) distance of 2.925 Å and a Pt(III)–Pt(III) distance of 2.695 Å were employed in these calculations.[16] The complexes $[Pt_2(pop)_4CH_3I]^{4-}$ and $[Pt_2(pop)_4{}^{13}CH_3I]$ have been treated in the C_{4v} point group. As seen in Figure 5, ν(Pt–Pt) is 156 cm^{-1} for $[Pt_2(pop)_4CH_3I]^{4-}$, while ν(Pt–C) is 489 cm^{-1} and shows a 14-cm^{-1} downshift with a $^{13}CH_3I$ isotope. The 170-cm^{-1} shoulder, which corresponds to the IR signal at 172 cm^{-1}, is assigned predominantly to the Pt–I stretch. Diagonal force constants are employed with the Pt–P, P–O, Pt–X, Pt–Pt, Pt–P–O, P–O–P, and P–Pt–P coordinates, along with (Pt–Pt; Pt–X) and (P–Pt–P; Pt–X) interaction constants. While the force constants involved with the bridging atoms are not varied among the complexes, the K(Pt–Pt) constants are differentiated for the Pt(II) and Pt(III) compounds. By adjusting the Pt–Pt and Pt–X force constants, a least-squares fit to the observed 19 Pt–Pt and Pt–X frequencies has been successfully accomplished.

The P–O stretches do not significantly couple with the low-frequency modes. The P–Pt–P bending and, to a lesser extent, the Pt–P–O bending coordinates, contribute and are allowed to vary over a 0.05–0.6 range between each cycle of the refinement procedure. A P–Pt–P bending vibration of A_{2u} symmetry is consistently found below 200 cm^{-1} and is assigned to the 178 and 172-cm^{-1} signals observed in the IR spectra of $[Pt_2(pop)_4I_2]^{4-}$ and $[Pt_2(pop)_4CH_3I_2]^{4-}$. The force field refinement is repeated to include these signals and the results with K(Pt–Pt) = 1.2 mdyn/Å and K(Pt–X) = 1.54, 1.36, and 1.03 mdyn/Å, respectively, are shown in Table II. Assignments are made by using the potential energy distributions as given. Additional frequencies with A_{1g}

symmetry are calculated at 758, 385, and 294 cm^{-1} and are assigned to the P–O stretch and Pt–P stretch and ring bend, respectively. Frequencies with A_{2u} symmetry are calculated at 923 and 372 cm^{-1} and are assigned to the P–O stretch and the Pt–P stretch. These frequencies do not significantly vary among the complexes. A value K(Pt–Pt) = 0.3 mdyn/Å reproduces the observed Raman frequency of 116 cm^{-1} for $[Pt_2(pop)_4]^{4-}$ and a value of ΔK(Pt–Pt) = 0.90 mdyn/Å between the binuclear Pt(III) and Pt(II) complexes in good agreement with the four-atom calculation. Metal–metal force constants that typically range between 1.0–1.3 mdyn/Å[20] have bond energies of approximately 40 kcal/mol, and those in the range 0.1–0.3 mdyn/Å have bond energies of 10–15 kcal/mol. Our results suggest that a partial single bond be assigned to $[Pt_2(pop)_4]^{4-}$ while a strong single bond characterizes the binuclear platinum(III) complexes. Consequently, while the analysis does not disagree with the simple MO description[4] for d^7 and d^8 binuclear platinum complexes there is not sufficient data to accurately determine the partial bond order of the $[Pt_2(pop)_4]^{4-}$ ion. The calculation, however, emphasizes that the observation of ν(M–M) does not automatically demand a metal–metal bond for structures of this kind.

The frequency lowerings of ν(Pt–Pt) in the $[Pt_2(pop)_4X_2]^{4-}$ complexes are attributed to kinematic coupling between the Pt–Pt and Pt–X stretching motions as indicated from the potential energy distribution in Table II. Contributions of Pt–X in ν(Pt–Pt) and Pt–Pt in ν(Pt–X), which increase with Cl < Br < I, cause changes in their normal modes. When mixing is small, as in $[Pt_2(pop)_4Cl_2]^{4-}$, the normal modes correspond to the Pt–Pt stretch (i.e., X ← Pt–Pt → X) and Pt–Cl stretch (i.e., ← X–Pt → ← Pt–X →); however, an in-phase and out-of-phase combination of these coordinates are calculated for ν(Pt–Pt) and ν(Pt–Br) or ν(Pt–I), respectively. Since resonance Raman transitions are intensified for normal modes that mimic distortions of the contributing excited electronic state,[21] the relative intensities of ν(Pt–Pt) and ν(Pt–X) in these complexes are predicted to vary. As seen in Figure 2 the intensity of ν(Pt–Pt) dramatically increases relative to ν(Pt–X) with Cl < Br < I. When mixing is small both normal modes produce a similar distortion pattern (namely, a lengthening of Pt–Pt and shortening of Pt–X or vice versa) and the intensities for ν(Pt–Pt) and ν(Pt–X) are expected to be comparable. When mixing is large ν(Pt–Pt) distorts by a lengthening of Pt–Pt and Pt–X distances while the distortion pattern of ν(Pt–X) remains the same. Thus, the intensity data, together with the normal coordinate analysis, suggest that the σ^* excited states have a geometry with longer Pt–Pt and Pt–X bonds than the ground state. Raman excitation profiles would be useful to further characterize the excited states.

Concluding Remarks

The vibrations ν(Pt–Pt) in the $[Pt_2(pop)_4X_2]^{4-}$ and $[Pt_2(pop)_4]^{4-}$ complexes are readily obtained by Raman spectral measurements. The K(Pt–Pt) force constants are a more sensitive indicator of the Pt–Pt bond strengths than the frequencies since the latter are influenced by bridging and axial ligand interactions. We have treated the axial ligand interactions by using a simple four-atom model, X–Pt–Pt–X, and find an increase in Pt–Pt bond strengths in binuclear Pt(III) as compared to Pt(II) complexes. We have found that the bridging ligand contributions to ν(Pt–Pt) become increasingly significant in $[Pt_2(pop)_4]^{4-}$ and can account for most of the restoring forces in that vibration. These results reemphasize the danger of assigning metal–metal bonds from vibrational data without considering the influences of ligand interactions.[22]

It may be appropriate to consider the phosphorescent data[8] of the $[Pt_2(pop)_4]^{4-}$ complex which show a ν(Pt–Pt) of 139 cm^{-1} in the excited triplet state. Fordyce et al.[8] estimated a Pt–Pt distance in the range 2.49–2.65 Å using a Franck–Condon analysis. An alternative approach is to apply the results of the four-atom calculation with Badger's rule,[23] incorporating the measured X-ray distances for the Pt–Pt separations in $K_4[Pt_2(pop)_4]\cdot 2H_2O$ and $K_4[Pt_2(pop)_4Cl_2]$. A Pt–Pt separation of 2.81 Å is calculated, corresponding to a 4% shrinkage of this bond in the excited triplet state. In light of the Pt–Pt distance of 2.695 (1) Å in $K_4[Pt_2(pop)Cl_2]$, it appears that the Franck–Condon analysis may overestimate the low shrinkage.[24]

Acknowledgment. We thank the donors of the Petroleum Research Fund, administered by the American Chemical Society, for the support of this research (Grant 11633AC3). We thank Professor Thomas G. Spiro for the use of the 171 Spectrophysics krypton ion laser. We thank Professor W. P. Schaefer for communication of his results prior to publication and Professor H. B. Gray for preprints of his work.

Appendix

The vibrational secular equation, given by

$$|\mathbf{GF} - \lambda| = 0 \qquad \text{(A1)}$$

where **G** and **F** are the kinetic and potential energy matrices, and $\lambda = 4\pi^2c^2\nu^2$ (c is the velocity of light, and ν, expressed in cm^{-1} is the vibrational energy), is applied to the linear X–Pt–Pt–X′ (X and X′ = Cl, Br, or I) system. Symmetry coordinates are defined as follows:

$$S_1 = r_{PtPt}$$

$$S_2 = (1/(2)^{1/2})(r_{PtX} + r_{PtX'})$$

$$S_3 = (1/(2)^{1/2})(r_{PtX} + r_{PtX'})$$

where r_{PtPt} is the PtPt stretching and r_{PtX} is the PtX stretching coordinates. The symmetrized **G** and **F** matrices

$$\mathbf{G} = \left\{ \begin{array}{lll} 1/\mu & -(2)^{1/2}/M_{Pt} & 0 \\ -(2)^{1/2}/M_{Pt} & 2/M_{Pt} & 0 \\ 0 & 0 & 1/\mu \end{array} \right\}$$

$$\mathbf{F} = \left\{ \begin{array}{lll} K_X + I_{XX'} & I_{PtX}/(2)^{1/2} & 0 \\ I_{PtX}/(2)^{1/2} & K_{Pt} & 0 \\ 0 & 0 & K_X - I_{XX'} \end{array} \right\}$$

separate the symmetric (2 × 2) asymmetric (1 × 1) blocks where $1/\mu = 1/M_X + 1/M_{Pt}$, K_{Pt} and K_X are diagonal force constants with r_{PtPt} and r_{PtX}, while I_{PtX} and $I_{XX'}$ are interaction constants between r_{PtPt} and r_{PtX}, and r_{PtX} and $r_{PtX'}$, respectively. The vibrations of Hg_2X_2 (X = Cl, Br, I) have been analyzed[25] with similar relationships.

Since there are more force constants than observed frequencies, unique solutions for the force constants are not possible. Assuming $I_{XX'} = 0$ and taking the observed ν(Pt–Pt) and ν(Pt–X) Raman signals, solutions for K_{Pt}, K_X, and I_{PtX} can be obtained by rearranging eq 1, using the symmetric **G** and **F** matrices. Plots of K_{Pt} vs. K_X for each $[Pt_2(pop)_4X_2]^{4-}$ complex gives an account of reasonable solutions as shown in Figure 6 where $0.1 < I_{PtX} < 0.4$ mdyn/Å. Solutions for $[Pt_2(pop)_4Br_2]^{4-}$ and $[Pt_2(pop)_4I_2]^{4-}$ are not attainable for I_{PtX} less than 0.11 and 0.15 mdyn/Å. The ^{195}Pt NMR measurements indicate similar Pt(III)–Pt(III) interactions

---

(20) See, for example: Ware, M. J. In "Essays in Structural Chemistry"; Downs, A. J., Long, D. A., Staveley, L. A. K., Eds.; MacMillan: London, 1971.

(21) Hirakawa, A. Y.; Tsuboi, M. *Science* (*Washington, D.C.*) **1975**, *188*, 359–361.

(22) Shriver. D. F.; Cooper, C. D., III *Adv. Infrared Raman Spectrosc.* **1980**, *6*, 127–157.

(23) Badger, R. M. *J. Chem. Phys.* **1935**, *3*, 710–714. The values d_{ij} = 1.934 Å and c = 0.75 mdyn Å^2 were determined by solving two simultaneous equations of the form: $r_{ij} = (c/K)^{1/3} + d_{ij}$, where r_{ij} and k are the atomic separations and force constants for the binuclear Pt(II) and Pt(III) complexes.

(24) Since completion of this work we have learned of a spectroscopic study on $[Pt_2(pop)_4]^{4-}$ which finds a Pt–Pt stretching frequency in the $^3A_{2u}$ state of 155 cm^{-1}. Using this value of 155 cm^{-1} rather than 139 cm^{-1} in our Badger's rule calculations results in a finding of 2.75 Å for the excited-state Pt–Pt separation. This distance is close to that of 2.71 Å found by these authors (S. F. Rice and H. B. Gray) from a vibrational analysis of the electronic spectrum.

(25) Durig, J. R.; Lau, K. K.; Nararajan, G.; Walker, M.; Bragin, J. *J. Chem. Phys.* **1969**, *30*, 2130–2139.

for these complexes and suggest equivalences in their K_{Pt} force constants. A narrow range, $1.69 < K_{Pt} < 1.85$ mdyn/Å, of solutions is seen which allow for a common K_{Pt} force constant. The choice of K_{Pt} does not alter the conclusion (as provided in the text) of the relative binuclear Pt(II) and Pt(III) bond strengths. Plots of K_{Pt} vs. I_{PtX} for these complexes (not shown) gives a near intercept (±0.02 mdyn/Å) of the curves with $K_{Pt} = 1.7$ mdyn/Å and $I_{PtX} = 0.16$ mdyn/Å and provides a reasonable solution. Values for K_{PtX} of 1.65, 1.45, and 1.16 mdyn/Å are readily obtained as shown in Figure 6. The calculated asymmetric ν(Pt–X) are 304, 206, and 161 cm^{-1} as obtained by $((K_{PtX})^{1/2}/\mu)/2\pi c$ and compare with the IR observations (295, 195, and 118 cm^{-1}). The large difference in ν(Pt–I) is attributed to mixing from an asymmetric ring mode and is discussed in the text.

Registry No. $K_4[Pt_2(pop)_4]$, 82135-51-1; $K_4[Pt_2(pop)_4Cl_2]$, 85335-49-5; $K_4[Pt_2(pop)_4Br_2]$, 82135-55-5; $K_4[Pt_2(pop)_4I_2]$, 85335-50-8; $K_4[Pt_2(pop)_4CH_3I]$, 82135-52-2.

Synthesis, Structure, and ^{195}Pt NMR Studies of Binuclear Complexes of *cis*-Diammineplatinum(II) with Bridging α-Pyridonate Ligands

L. Steven Hollis and Stephen J. Lippard*†

Contribution from the Department of Chemistry, Columbia University, New York, New York 10027. *Received November 15, 1982*

Abstract: With ^{195}Pt NMR spectroscopy, several products formed in the reaction of *cis*-$[Pt(NH_3)_2(H_2O)_2]^{2+}$ with α-pyridone (C_5H_4NHO) have been identified in solution at pH 4.2. These complexes, present in the aqueous solution from which the *cis*-diammineplatinum α-pyridone blue is ultimately obtained, include $[Pt(NH_3)_2(OH)]_2^{2+}$, $[Pt(NH_3)_2(OH)]_3^{3+}$, *cis*-$[Pt(NH_3)_2(C_5H_4NOH)(H_2O)]^{2+}$, *cis*-$[Pt(NH_3)_2(C_5H_4NOH)_2]^{2+}$, and the head-to-head and head-to-tail α-pyridonate-bridged dimers $[Pt_2(NH_3)_4(C_5H_4NO)_2]^{2+}$. Crystals of the last two complexes were obtained from the reaction by careful control of the pH. A rational synthesis of the head-to-tail isomer was achieved from dimerization of *cis*-$[Pt(NH_3)_2(C_5H_4NOH)(H_2O)](NO_3)_2$. X-ray diffraction studies revealed the structure of the head-to-tail dimer, $[Pt_2(NH_3)_4(C_5H_4NO)_2](NO_3)_2\cdot 2H_2O$, to contain two α-pyridonate ligands bridging two *cis*-diammineplatinum(II) units with a Pt–Pt distance of 2.898 (1) Å. The head-to-head platinum(II) isomer dimerizes with itself in the crystal lattice to form a tetramer, $[Pt_2(NH_3)_4(C_5H_4NO)_2]_2(NO_3)_4$, that is held together by bridging α-pyridonate ligands and by stacking and intercation hydrogen-bonding interactions. The structure of this yellow complex is strikingly similar to that of the α-pyridone blue except for longer Pt–Pt distances, 2.877 (1) and 3.129 (1) Å vs. respective values of 2.775 (1) and 2.877 (1) Å in the blue, owing to differences in metal–metal bond order for the two complexes.

During the past decade the scope of aqueous platinum(II) chemistry has undergone a significant expansion with the discovery and exploration of the antitumor properties of *cis*-diamminedichloroplatinum(II), *cis*-DDP.[1] The growth in this area is presently being maintained by the widespread success that *cis*-DDP is finding in the clinical treatment of human cancer.[1c] One of the directives of work in this area continues to be the development of an understanding of the mechanism of drug action. Since the antitumor activity of *cis*-DDP is thought to result from the inhibition of cellular replication, induced by the interaction of the drug with DNA,[2] the study of the reactions of *cis*-DDP with nucleic acids and their constituents has become an active area of investigation.[3]

The chemistry of platinum–nucleotide interactions is a complex and diversified field of study. The reaction of *cis*-DDP or the aquated form of the complex, *cis*-$[Pt(NH_3)_2(H_2O)_2]^{2+}$, with free or substituted pyrimidine bases, leads to a variety of products[3-15] that can be classified according to the number of platinum atoms contained in the product molecule. A multiformity of simple mononuclear and binuclear platinum complexes of free and substituted uracil, thymine, and cytosine has been isolated and studied by ^{1}H NMR, vibrational spectroscopy, and X-ray crystallography.[5-15] In these compounds the platinum binds either, in mononuclear complexes, to one of the heterocyclic nitrogens (N1, N3) of the pyrimidine base or, in pyrimidine-bridged bi-

---

† Address correspondence to this author at the Department of Chemistry, Massachusetts Institute of Technology, Cambridge, MA 02139.

(1) (a) Rosenberg, B.; Van Camp, L. *Cancer Res.* **1970**, *30*, 1799. (b) Paoletti, C., Ed. *Biochemie* **1978**, *60*, 915–965. (c) Prestayko, A. E.; Crooke, S. T.; Carter, S. K., Eds. "Cisplatin, Status and New Developments"; Academic Press: New York, 1980. (d) Lippard, S. J. *Science (Washington, D.C.)* **1982**, *218*, 1075–1082.

(2) Roberts, J. J.; Thompson, A. J. *Prog. Nucleic Acid Res. Mol. Biol.* **1979**, *22*, 71.

(3) For a review see: Barton, J. K.; Lippard, S. J. In "Nucleic Acid–Metal Ion Interactions"; Spiro, T. G., Ed.; Wiley: New York, 1980; p 32.

(4) (a) Davidson, J. P.; Faber, P. J.; Fischer, R. G., Jr.; Mansy, S.; Peresie, H. J.; Rosenberg, B.; Van Camp, L. *Cancer Chemother. Rep.* **1975**, *59*, 287. (b) Lippert, B. *J. Clin. Hematol. Oncol.* **1977**, *7*, 26.

(5) (a) Lippert, B.; Pfab, R.; Neugebauer, D. *Inorg. Chim. Acta* **1979**, *37*, L495. (b) Lippert, B. *Ibid.* **1981**, *55*, 5. (c) Lippert, B. *Ibid.* **1981**, *56*, L23. (d) Lippert, B.; Neugebauer, D. *Ibid.* **1981**, *46*, 171. (e) Lippert, B.; Schubert, U. *Ibid.* **1981**, *56*, 15. (f) Lippert, B.; Neugebauer, D. *Inorg. Chem.* **1982**, *21*, 451. (g) Pfab, R.; Jandik, P.; Lippert, B. *Inorg. Chim. Acta* **1982**, *66*, 193.

(6) Lock, C. J. L.; Peresie, H. J.; Rosenberg, B.; Turner, G. *J. Am. Chem. Soc.* **1978**, *100*, 3371.

(7) Wu, S.-M.; Bau, R. *Biochem. Biophys. Res. Commun.* **1979**, *88*, 1435.

(8) (a) Lippert, B.; Lock, C. J. L.; Speranzini, R. A. *Inorg. Chem.* **1981**, *20*, 808. (b) Faggiani, R.; Lippert, B.; Lock, C. J. L. *Ibid.* **1982**, *21*, 3210.

(9) Faggiani, R.; Lippert, B.; Lock, C. J. L.; Pfab, R. *Inorg. Chem.* **1981**, *20*, 2381.

(10) Lippert, B.; Lock, C. J. L.; Speranzini, R. A. *Inorg. Chem.* **1981**, *20*, 335.

(11) Faggiani, R.; Lippert, B.; Lock, C. J. L. *Inorg. Chem.* **1980**, *19*, 295.